Thermodynamic structure of the marine atmosphere over the region 80–87°E along 13°N during August (phase II) BOBMEX-99

SAVITA B MORWAL and P SEETARAMAYYA

Indian Institute of Tropical Meteorology, Dr. Homi Bhabha Road, Pashan, Pune 411 008, India
e-mail: morwal@tropmet.res.in

Thermodynamic structure of the marine atmosphere in the region between 80 and 87°E along 13°N over the Bay of Bengal was studied using 13 high resolution radiosonde profiles from surface −400 hPa collected onboard ORV Sagar Kanya during the period 27th – 30th August, during BOBMEX-99. Saturation point concept, mixing line analysis and conserved variable diagrams have been used to identify boundary layer characteristics such as air mass movement and stability of the atmosphere. The results showed relatively dry air near the ocean surface between 1000 and 950 hPa. This feature is confirmed by the conserved θ_v structure in this layer. Further, θ_v seldom showed any inversions in this region. The θ_e and θ_{es} profiles showed persistent low cloud layers between 900 and 700 hPa. The conserved variable diagrams $(\theta_e - q)$ showed the existence of double mixing line structures approximately at 950 and 700 hPa levels.

1. Introduction

The Bay of Bengal Monsoon Experiment (BOBMEX-99) was undertaken to improve our understanding of monsoon circulation over the Bay (Sikka and Sanjeeva Rao 2000). The objectives included study of the vertical stability of the marine atmospheric boundary layer (MABL) during different phases of organized convection. Bhat *et al* (2001) have summarized the details of the above experiment and described some of the initial results obtained during the experiment at two stationary locations in the Bay at 13°N, 87°E (south Bay) and 17.5°N, 89°E (north Bay). High resolution radiosondes were launched for the first time in the north Bay during BOBMEX. From these data, it has been possible to derive important information about the variation of the vertical stability of the atmosphere. It is important to note here that the above high resolution observations were also taken along the 13°N latitude between 80°E and 87°E at an interval of 6 hours covering about 13 radiosondes during the last few days of

phase II of BOBMEX-99 i.e., from 27th to 30th August, 1999. Using this data set we study the dynamic and thermodynamic processes related to convective activity over this region.

2. Data and method of analysis

Aerological observations collected during the end of phase II (vide Bhat 2001) from 27th – 30th August 1999 i.e., when the ship was moving along constant latitude 13°N, have been used. During the course of observations the ship moved from an open marine environment towards the coast along the latitude 13°N from 87°E to 80.79°E. The 6-hourly radiosonde upper air data collected during this time have been used to investigate some of the characteristic features of the thermodynamic structure of the Marine Atmospheric Boundary Layer (MABL). Also, 3-hourly surface meteorological parameters (surface pressure, dry-bulb temperature, dew point temperature, sea surface temperature, wind speed, wind direction and total cloud

cover) have been used to explore the diurnal variation of the surface parameters in the surface layer.

The study area has been divided into three regions based on the distribution of the mean sea level pressure (figure 2a) and the total cloud amount (figure 2b). They are: region I (87° to 85°E), in which the pressure in general decreased from east to west with a steep change in the cloud amounts varying between 4 and 8 octa i.e., a region of partly cloud cover; region II (85° to 82°E), in which the pressure increased westwards and complete overcast sky (8 octa) and region III (west of 82°E), in which pressure remained constant with partial overcast sky (7–8 octa).

In the present study 13 radiosonde soundings have been analyzed for the period of observation 27th – 30th August 1999. The data of air temperature (T) and dew point temperature (T_d) were obtained from very high resolution (at an interval of 5 hPa) radiosonde soundings from surface up to 400 hPa level at an interval of 6 hours. These soundings have been used to compute potential temperature (θ), virtual potential temperature (θ_v), equivalent potential temperature (θ_e), saturated equivalent potential temperature (θ_{es}) and mixing ratio (q). The height of the Lifting Condensation Level (LCL) has been computed using surface values of air temperature and dew point temperature.

The parameter P^*, saturation pressure deficit, was computed as $p_{SL} - p$, where p is the pressure of the air parcel at the described level and p_{SL} is the saturation level pressure. P^* indicates the lack of saturation in the layer p to p_{SL}. It is positive in the cloudy region and negative in the unsaturated region. Thus, high negative values of P^* are always associated with the dry regions or regions with low relative humidity. The vertical distribution of P^* is very useful to delineate the different sub layers such as surface layer, mixed layer, cloud layer and overlying stable or inversion layer in the MABL (Betts 1982; Morwal 2000).

When two air parcels of different characteristics mix together the characteristics of the new mixed air parcel can be shown on $T - \phi$ gram by using the method of mixing line analysis. The Saturation Point (SP) of the mixed parcel can be computed by using the properties of an individual air parcel with the formulae described elsewhere (Morwal 1998). All the SPs computed lie on a line called mixing line (Betts and Albrecht 1987). On $T - \phi$ grams the mixing line is somewhat curved. However, the mixing lines can also be represented on the conserved variable diagrams $(\theta_e - q)$. On these diagrams the mixing lines are straight lines and they are very useful to understand the physical and thermodynamical processes in the MABL. Generally, in the MABL shallow cumulus clouds do not penetrate through the cloud topped stable layer or clouds which do not produce the rain, are represented by a single mixing line.

3. Synoptic weather conditions over the Bay of Bengal region

Figure 1(a–d) shows the four synoptic weather charts at 0300 UTC (0830 IST) from 27th to 30th August respectively. In figure 1(a–d) the ship track is shown by a straight line joining Chennai (CNN) and an open circle at 87°E in the ocean along 13°N. The 6-hourly position of the ship (open circles) from east (87°E) to west (80.79°E) during the period of observation is also shown in figure 1(e) (inset below left corner) along with boundaries of regions I, II and III. Figure 1(a–d) depicts a predominant well-marked intense low pressure area, L, with a concentric closed circular isobar 1004 hPa on 27th August and 1002 hPa on 28th August over the northwest Bay of Bengal at 20°N, 90°E and gracing the north Orissa coast. On 29th – 30th August, this system moved northwestward to the adjoining land area over Orissa and West Bengal. The other main features in the above charts are the trough lines projecting outside from the low (dashed lines) and the ridges (zigzag lines) on the peripheries of the low. The prominent among the troughs are (i) the semi-permanent monsoon trough over central India and (ii) the trough parallel to the east coast (Coromandal coast) in the western Bay. The southern end of this trough shifted westward to the neighbouring land areas of north Andhra Pradesh and Orissa from 27th to 30th August. Following movement of the low and troughs, the ridge over the Andaman Sea, on 27th August, also shifted westward to the south of 13°N. The gradient of pressure was 4 hPa from 13°N to the centre of low on 27th, 28th and 29th August and 6 hPa on 30th August. There was southwesterly wind (10–20 knot) across the east-west isobars. All the above synoptic weather features over the Head Bay had a bearing on the variation of the observed meteorological parameters (figure 2). The 1008 hPa isobar is seen to be running along 13°N on 27th and 28th August and this isobar was replaced by 1006 hPa isobar on 29th August and the same isobar (1008 hPa) has again returned back to the above latitude on 30th August. This type of to and fro motion from north to south and back at 13°N seems to have rapidly altered the surface and upper wind field over the study area. The monsoon was active in the region north of 13°N and over the Indian sub-continent during the period under study. Winds were generally southwesterly offshore and northwesterly near the coastline and
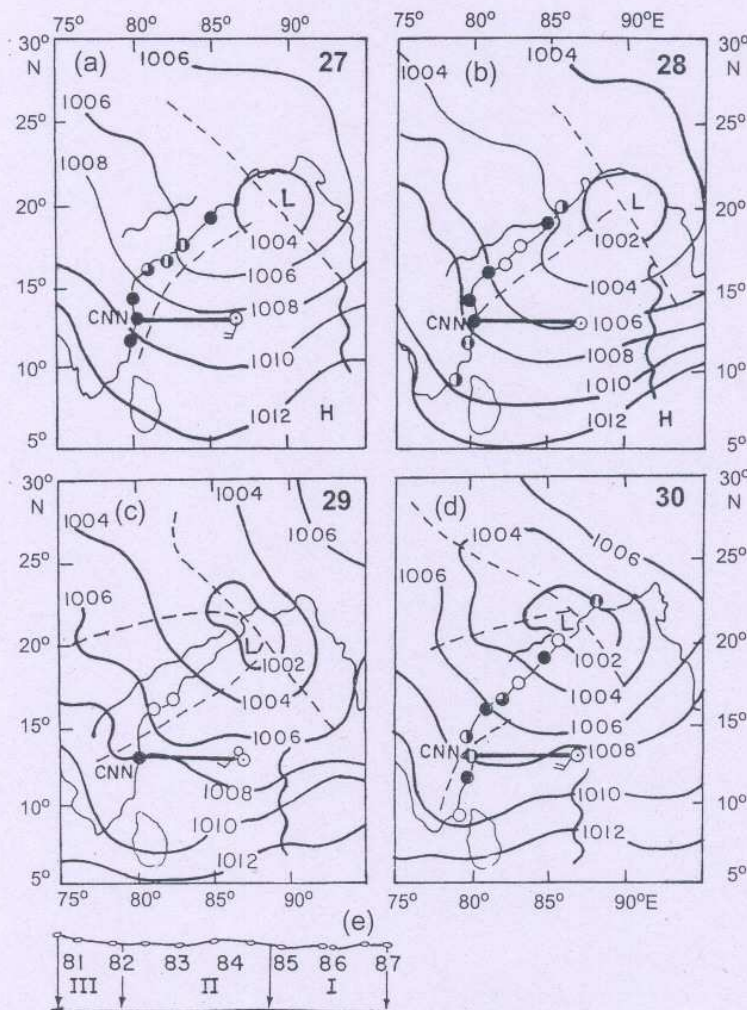
Figure 1. Surface synoptic weather charts for (a) 27th August (b) 28th August (c) 29th August (d) 30th August 1999 at 0830 IST. The dashed line indicates the trough and zigzag line represents the ridge. (e) Position of the ship in the three regions.

strong. During this period, on some occasions, precipitation was observed along the ship track. The total cloud amount over the region was generally 4–8 octa.

4. Results and discussion

4.1 *Distribution of surface meteorological parameters*

Figure 2 illustrates the distribution of 3-hourly mean sea level pressure (P, hPa), T, T_d, sea surface temperature (SST, °C), wind direction (dd, deg), wind speed (ff, m sec^{-1}), total cloud amount (CA, octa) and height of the lifting condensation level (LCL, hPa) for the period from 06 IST of

27th August to 12 IST of 30th August along 13°N from 87 to 80.79°E (the scale on abscissa is 0, 24, 48 and 72 hours in series starting from 00 IST of 27th August). Figure 2(a) shows the distribution of P and LCL along 13°N during the period of observation. Note that the P field shows two types of oscillations. The first oscillation corresponds to a semi-diurnal pressure wave and the second oscillation corresponds to synoptic pressure wave due to the ongoing developing low pressure area over the northwest Bay of Bengal (figure 1a–d) along the West Bengal-Orissa coast line.

The pressure decreased from 87°E to 85°E and after that showed a gradual increase in the region west of 85°E. This is indicative of the influence of the prevailing low pressure area in the northwest Bay off the West Bengal-Orissa coast on 27th

August and its subsequent movement in a north-westerly direction from 28th August onwards. Thus when the low-pressure area is close to the ship the pressure is low and as the system moves away, the pressure gradually increases. Secondly, the total cloud amount (figure 2b) varied between 4 and 8 octa (partially cloudy; region I) in the region east of 85°E, 8 octa (overcast; region II) in the region between 85°E and 82°E and between 7 and 8 octa (partly overcast; region III) in the region west of 82°E. The linear inclined line from left to right in this figure (2b) illustrates the positions of the longitudes at the respective times of observations. Thus, based on the distribution of surface pressure and the total cloud amount the observational area is divided into three regions namely region I (east of 85°E), region II (85–82°E) and region III (west of 82°E). The three regions are marked by vertical dotted lines in figure 2(a–d). Also, horizontal lines in figures 2(a), 2(c), and 2(d) are drawn to illustrate the average value and trend of the concerned parameter.

In figure 2(a), the LCL height (in pressure units, hPa) varied from 981 hPa to 946 hPa with a mean height of about 963 hPa (horizontal solid line). In region I the LCL is in general above the mean LCL except at a few hours. These hours are associated with rainfall activity (confirmed from continuous rainfall data recorded onboard ORV Sagar Kanya) and hence the LCL is observed at lower levels. Region II is represented by the LCL values oscillating around the mean LCL line whereas the LCL is below the mean in region III.

In general, the SST varied around 28.5°C (figure 2c). In figure 2(c) the solid and dashed horizontal lines represent the mean air temperature (28°C) and dew point temperature (25°C) respectively. Dew point temperature fluctuates around 25°C and the atmosphere is dry at the surface in all the three regions. The air temperature is above 28°C in region I and below 28°C in regions II and III. The sudden drop in air temperature on few occasions (in all the three regions) is associated with rainfall episodes (seen from continuous rainfall records). It is noticed that when the air temperature is very close to SST the LCL is found at lower levels.

Figure 2(d) shows the 3-hourly distribution of surface wind direction (*dd*, solid line with solid circles) and wind speed (*ff*, solid line with open circles). From this figure it is evident that over the southern Bay of Bengal during the period of observation the wind speed varied between 6 and 15 m sec^{-1} and matched with climatological values (Hastenrath and Lamb 1979). The wind direction was more or less constant. It varied within 30 degrees around the southwest on some occasions following the disturbance. Also the variation of wind speed from 87°E to 80.79°E indicates that there is a gradual decrease of wind speed when the ship is moving from marine atmosphere in the east towards the coast in the west. Similar results were also reported by Swain *et al* (2001), who utilized the wind observations collected over the ship INS Sagardhwani during July–August of BOBMEX-99 over the southcentral Bay of Bengal (13°N, 89°E). However the wind speed varied in the three regions, with a high speed (> 12 m sec^{-1}) in region I and moderate to low (7.5–10 m sec^{-1}) in regions II and III. There are some critical sudden changes in both the speed and direction at some times in the wind field. These changes are found to be due to downdrafts under clouds.

4.2 *Thermodynamic structure of the marine atmosphere*

4.2.1 *Region I*

Figure 3 illustrates the vertical profiles of q, θ_v, θ_e and θ_{es} from surface up to 400 hPa level for the radiosonde profiles, taken in region I of the study area. These are representative of the marine atmosphere where the total cloud amount typically varies from 4 to 8 octa, a weak convective zone. The corresponding $\theta_e - q$ profile diagrams are shown in figure 6. During the period from 1130 IST of 27th August to 1730 IST of 28th August, there are about 6 radiosonde ascents in the area of study and are denoted from (a) to (f) in figure 3. Among the six profiles the three central profiles (figures 3b, 3c and 3d) are taken in the region where the total cloud amount is low (4 to 6 octa) and the extreme three profiles of figures 3(a), 3(e) and 3(f) are taken in the region where total cloud cover is 8 octa. Moreover this region had high wind speed (> 10 m sec^{-1}). It is interesting to note that none of the above profiles were alike/same. However, the q profiles in general showed a gradual decrease with height from surface up to 400 hPa level. Nevertheless there are layers of constant q in the middle levels where these layers are generally affected by the low cloud decks present in the atmosphere (e.g., figures 3a, 3d and 3e). The θ_v profiles show a thin surface layer of thickness 50–90 m (i.e., 5 to 9 hPa) at the surface at all places along the section in region I. The layer is characterized by a decrease of q with height (vide q curves) and more than normal adiabatic lapse rates (> 0.03 K m^{-1}). The profile at 85.81°E showed a super adiabatic lapse rate (0.2 K m^{-1}) and this steep lapse rate had associated with a pronounced decrease in the q value with height. Mollor (Haltiner and Martin 1957) has shown that whenever the lapse rate γ increases (decreases) in the vertical through the reference level, more (less) than the normal cooling tend to
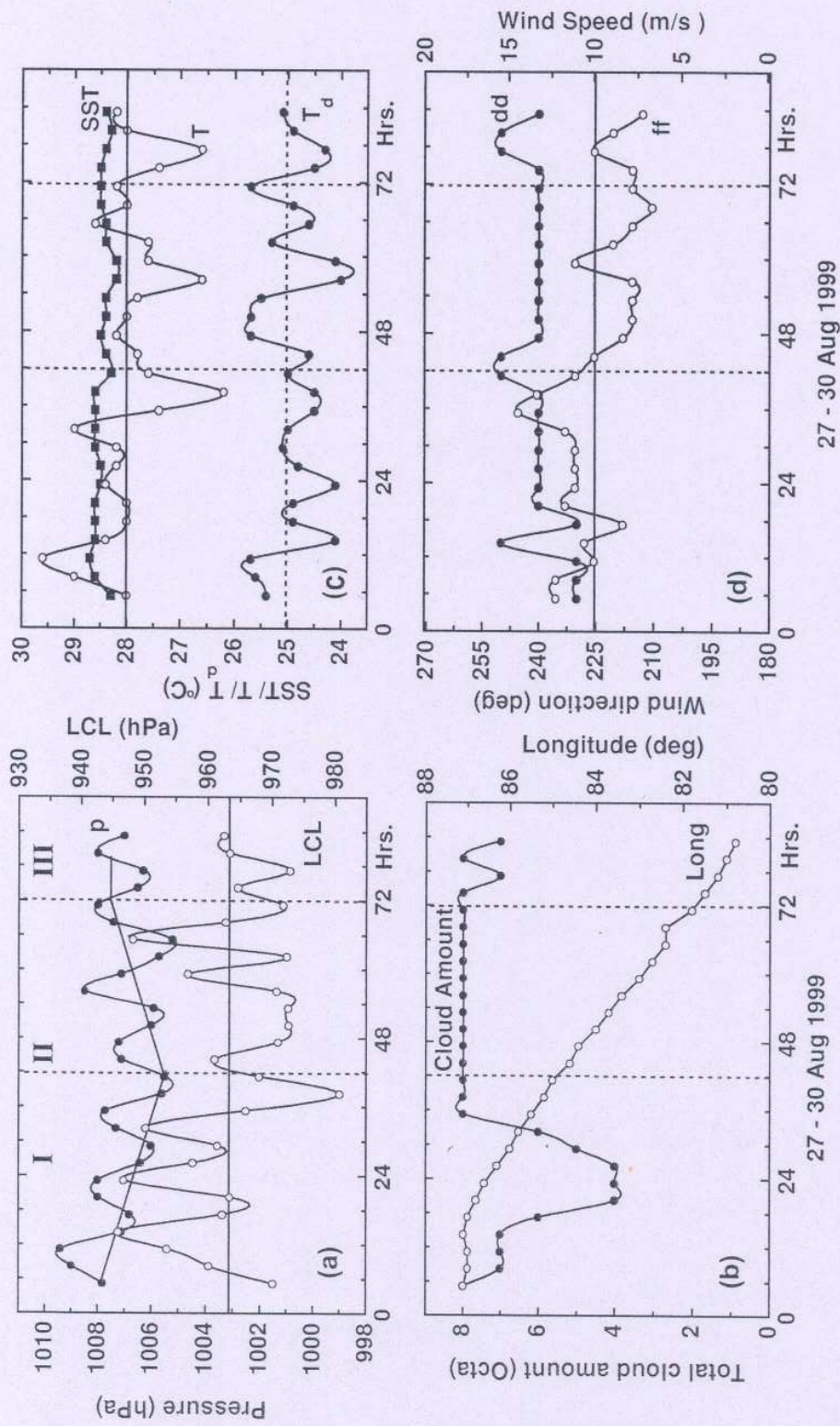
Figure 2. Daily march of the surface parameters in the regions I, II and III. (a) Surface pressure (p) and lifting condensation level (LCL). (b) Total cloud amount and longitude. (c) Sea surface temperature (SST), air temperature (T) and dew point temperature (T_d). (d) Wind speed (ff) and wind direction (dd).
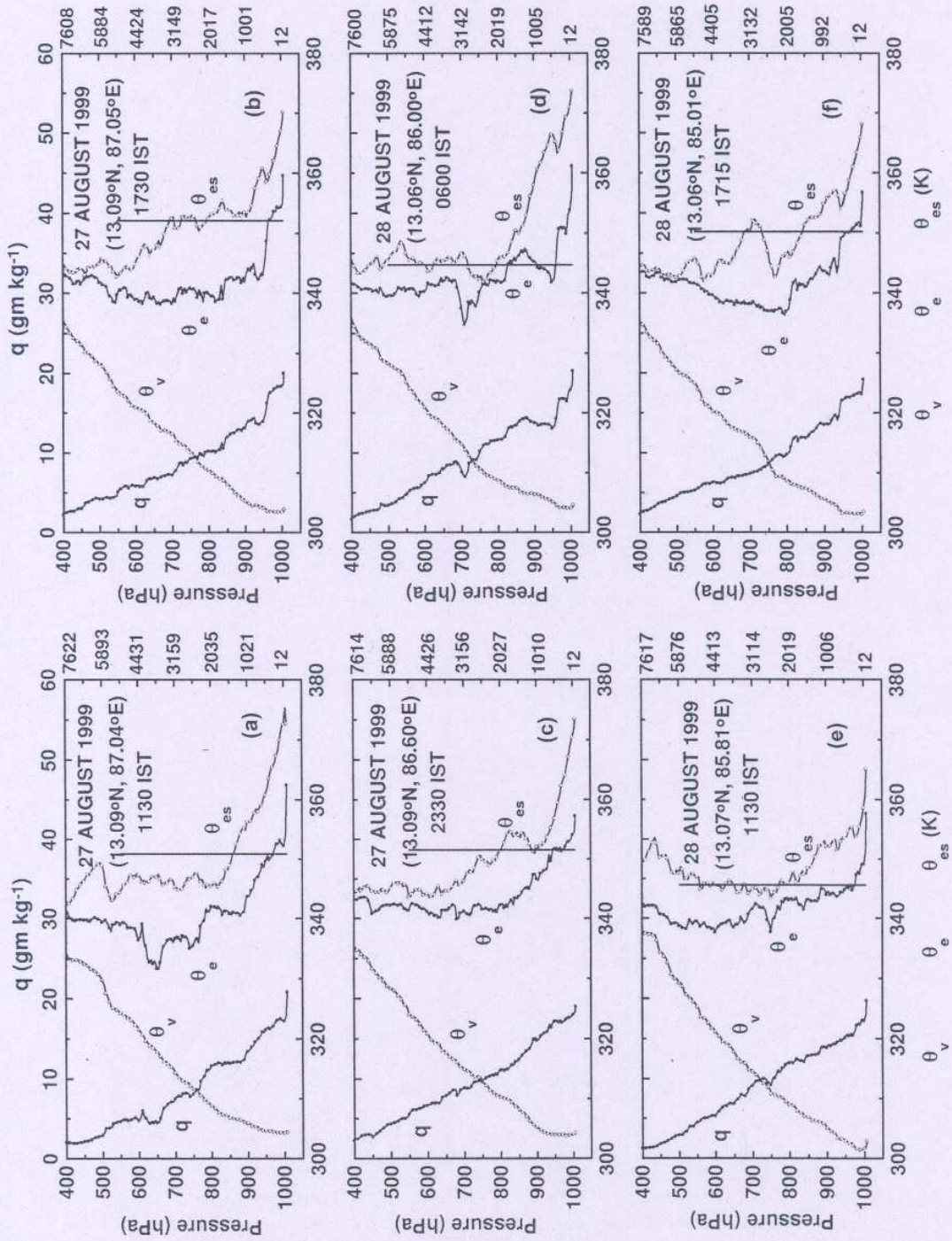
Figure 3. Vertical distribution of q, θ_v, θ_e and θ_{es} for the 6-hourly radiosonde soundings over region I. The vertical straight line is drawn from the θ_e at LCL level. In each figure on the Y-axis pressure levels are marked on the left side and the corresponding heights are indicated on the right side.

occur at the level. However, one must also consider the effect of the variation of specific humidity. Assume now that no marked vertical variation in lapse rate occurs. Thus a marked decrease of specific humidity (q) through the reference level is likely to be associated with greater than normal cooling. However, an increase of q with height would normally lead to less than normal cooling. Therefore, it is presumed that the above process of 'q' variation with height might be operating. Similar virtual potential temperature lapse rates in the surface layer were also seen in figures (vide figures 1 and 2, page 900) of Venkata Ramana *et al* (1999), in the Indian Ocean during INDOEX. Bhat (2001) has also reported a similar feature while examining the vertical distribution of CAPE (Convectively Available Potential Energy) at $17.5°N, 89°E$ in the same month during BOBMEX-99. He concluded that the CAPE decreases with height and exhibits a large difference in CAPE between the surface and 1000 hPa suggesting the existence of a very shallow ($\sim < 50$m) surface layer where energy (entropy) decreases rapidly with height, somewhat similar to what happens on land on sunny days. In the present case no radiation is present due to overcast sky in the region. The θ_v also showed a sub cloud layer (or mixed layer) just above the surface layer with thickness 300 to 900 m (i.e., top of the sub cloud layer varies from 970 to 910 hPa). This sub cloud layer was characterized by a constant θ_v values (approximately) with height where the air mass is very well mixed and in which the θ_v is conserved. The property by which the θ_v is conserved in the sub cloud layer is otherwise known as the 'mixed layer' (Bhat *et al* 2000). Over the oceans this mixed layer plays an important role, and acts as a link between the surface layer and the free atmosphere. It carries upward the properties of the surface layer from the surface and gives them to the free atmosphere at the top of the mixed layer. Thus the mixed layer undergoes a transient mixing at both the ends of this layer. This type of mixing leads to thin interface layers between the surface layer and the mixed layer one near the surface and another at the top of the mixed layer and below the free atmosphere. These layers can be identified as thin transition layers at the bottom and top of the mixed layer.

The vertical profiles of θ_e and θ_{es} show the convective activity over the area. The vertical straight line in figures 3(a–f), that start, from θ_e at LCL (~ 960 hPa) on the θ_e curve and passing through the θ_{es} curve, is known as a constant θ_e line (the path of the non-entraining air parcel, Betts and Albrecht 1987). This line judges qualitatively the characteristic development of the

convective clouds/convection over the region and also the convective stability (buoyancy) of the atmosphere.

On the basis of the low level stability, Kloesel and Albrecht (1989) have classified the radiosonde soundings to examine the various types of convection and have given three types of idealized profiles based on θ_e and θ_{es} and the path of the non-entraining air parcel. They are: (**i**) Inversion sounding, (**ii**) high θ_e sounding and (**iii**) low θ_e sounding. In case of an inversion sounding the rising parcel from LCL (with LCL temperature) intersects the θ_{es} curve below 600 hPa. Such a kind of inversion is generally found in the region of fair weather cumulus and stratus clouds. In case of high θ_e soundings the rising parcel is buoyant positively right up to 600 hPa and leads to an unstable condition and deep convection. In the case of low θ_e sounding the parcel is negatively buoyant above the LCL to at least up to 600 hPa level and leads to the stable conditions and suppressed convection. The above method can be applied over land as well as over oceanic regions to characterize the differences in the thermodynamic structure of the boundary layer.

In the present study, none among the six profiles of region I has shown inversions except in one case at 1715 IST of 28th August, at $85.01°E$ (figure 3f). At this position the inversion occurred around 700 hPa. Hence this sounding can be treated as an inversion sounding. Further it is noted that this sounding has been taken over an overcast area where low and medium clouds were present and the surface q represents only 19.3 gm kg^{-1}. It is felt here that the clouds present at the time of observation are of fair weather cumulus and stratus type. Out of the remaining five soundings most of the profiles showed low level stability and upper level instability indicating suppressed convection.

The profile taken at 2330 IST of 27th August near $86.6°E$ (figure 3c) seems to be the only one profile that fulfils the criterion of deep convection. This profile is seen to be taken in the area of partly cloudy (4 octa) conditions and surface specific humidity is relatively low (19.1 gm kg^{-1}) as compared to the other surrounding profiles (~ 20 gm kg^{-1}). The profiles of q, θ_v, θ_e and θ_{es} at this location are quite different from the profiles of other positions. These profiles indicate relatively dry convection (Seetaramayya *et al* 2001). The q decreased linearly from surface up to 400 hPa level. The θ_e decreased slowly from 1000 hPa to 700 hPa and thereafter remains constant at 340 K. The θ_{es} curve also followed θ_e curve except in the layer between 900 and 800 hPa where the θ_{es} showed a weak inversion.

The profile taken at 0600 IST of 28th August (figure 3d), near 86°E showed a structure similar to other profiles. There were two levels of distinct θ_e minima at 960 and 710 hPa. The latter level may be treated as the top of the boundary layer and the former level may be treated as the top of the mixed layer near the surface. The levels of the above two minima coincide with the θ_{es} maxima in the θ_{es} curve.

It is interesting to note that all the above θ_e and θ_{es} profiles seldom show any pronounced subsidence from the top of the atmosphere.

4.2.2 Region II

Figure 4 (a–d) illustrates the thermodynamic properties of q, θ_v, θ_e and θ_{es} over region II which was a region of high total cloud cover (8 octa). In this diagram the q profiles show a general decreasing tendency with height but there are intermittent fluctuations along the mixed and cloudy layers and a steep decrease above the cloud top i.e., above 600 hPa. The values of q at the surface in the four soundings are 20.3, 20.5, 21.0 and 18.5 gm kg^{-1} (table 1) and those at 1000 hPa are 17.9, 19.3, 17.0 and 16.5 gm kg^{-1} respectively. This implies a decrease of about 2–3 gm kg^{-1} water vapour between surface and 1000 hPa. The constancy of θ_v showed mixed layer (sub cloud layer) depth up to 920, 890, 940 and 920 hPa in figure 4 (a) to (d) respectively. Further the θ_e and θ_{es} profiles showed a different thermal structure from region I.

In figure 4(a–d), only one sounding (figure 4b) fulfilled the condition of deep convection and the remaining three soundings showed shallow convection. In figure 4(a) the θ_e minimum was seen at 770 hPa and the θ_{es} maximum was seen only at 880 hPa which did not match with the θ_e minimum. The MABL height lies in between these two levels. There were several θ_{es} maxima above 750 hPa level and both the θ_e and θ_{es} curves run upward close to each other. This implies that the air mass is quite well mixed and saturated. The profiles of θ_e and θ_{es} of figure 4(b) seldom show any well defined θ_e minimum and θ_{es} maximum. However there was a typical minimum and maximum in θ_e and θ_{es} at 890 and 870 hPa respectively. The secondary θ_e minimum and θ_{es} maximum was at 680 hPa level. The $\theta_e = 340$ K from 750 to 460 hPa and the corresponding θ_{es} is 345 K. Further from figure 4(c) the θ_e minima were seen at 960 and 730 hPa and the θ_{es} maxima coincided with the θ_e minima. There were two θ_e minima and four θ_{es} maxima in figure 4(d). The θ_e minima were at 940 and 770 hPa and the θ_{es} maxima were at 940, 790, 660 and 470 hPa levels respectively. Both the minima and maxima were not coinciding with each other in

this case. The LCL heights in figure 4(a–d) are at 964.4, 965.6, 967.2 and 937.5 hPa (table I) levels respectively. The pseudoadiabat (constant θ_e straight line) rising upward from θ_e at LCL level cuts the θ_{es} at 790 hPa in figure 4(a), 670 hPa in figure 4(c) and 600 hPa in figure 4(d) and does not cut the θ_{es} curve in figure 4(b). The θ_e and θ_{es} profiles are on either side of the pseudoadiabat below the point of intersection in figure 4(a), 4(c) and 4(d) and both curves are to the left of pseudoadiabat in figure 4(b). The areas where both the θ_e and θ_{es} curves either tend to decrease with height or come close to each other show a state of convective conditional instability. Such processes are mostly present in the cloud layer in all the above figures.

The θ_e and θ_{es} profiles of figures 4(b) (deep convection) and 4(d) (suppressed convection) are similar to those illustrated by Kloesel and Albrecht (1989) for high θ_e group and the low θ_e group. Both profiles were taken under the overcast conditions. Yet each one of them showed independent characteristics based on the humidity available over the area. The profiles showed medium and high clouds rather than low level stratus or cumulus clouds all through the length of the cruise along 13°N in region II. This implies that these clouds were of advective type rather than the locally generated cumulus clouds.

4.2.3 Region III

It is seen from figure 5(a–c) that the vertical distribution of q changed considerably from other two regions in the layer between 800 and 400 hPa and there was a pronounced q gradient (relatively dry) with height (varying between 2 and 10 gm kg^{-1}). The q curve exhibited rapid changes between 700 and 600 hPa levels. The reason for these changes is not yet known. The surface and 1000 hPa values of q over the three soundings respectively were 20.4, 18.2, 20.4 and 17.8, 16.3, 18.4 gm kg^{-1} for region III (table 1). The values of q in the surface as well as 1000 hPa were observed to be lowest in figure 5(b) as compared to those in figures 5(a) and 5(c).

Examination of the structure of the profiles of θ_e and θ_{es} showed substantial dryness in the marine boundary layer over region III by exhibiting a wide gap between both the curves in all the figures (figure 5(a–c)) from 1000 to 550 hPa except at 670 hPa in figure 5(c) where the curves of θ_e and θ_{es} came close to each other. Above the level 550 hPa they tended to meet each other. The dryness was more pronounced in the mixed layer between 1000 and 980 hPa. Both the θ_e and θ_{es} curves exhibit multiple minima and maxima. The levels of θ_e minima in figure 5(a) were at 970 and 600 hPa (MABL

Table 1. *Thermodynamical parameters in the MABL for each 6-hourly radiosonde ascent over regions I, II and III during the period 27th – 30th August 1999.*

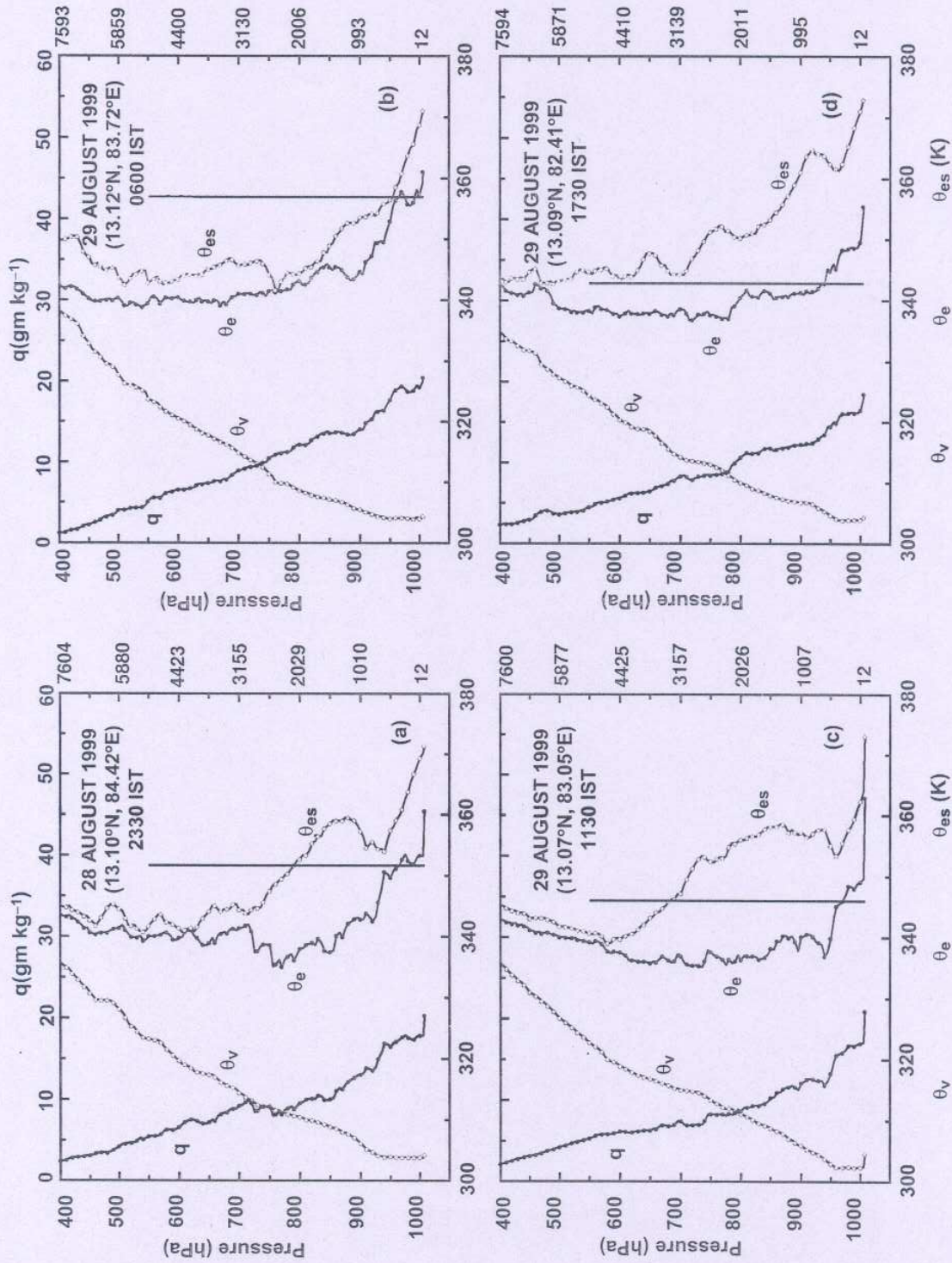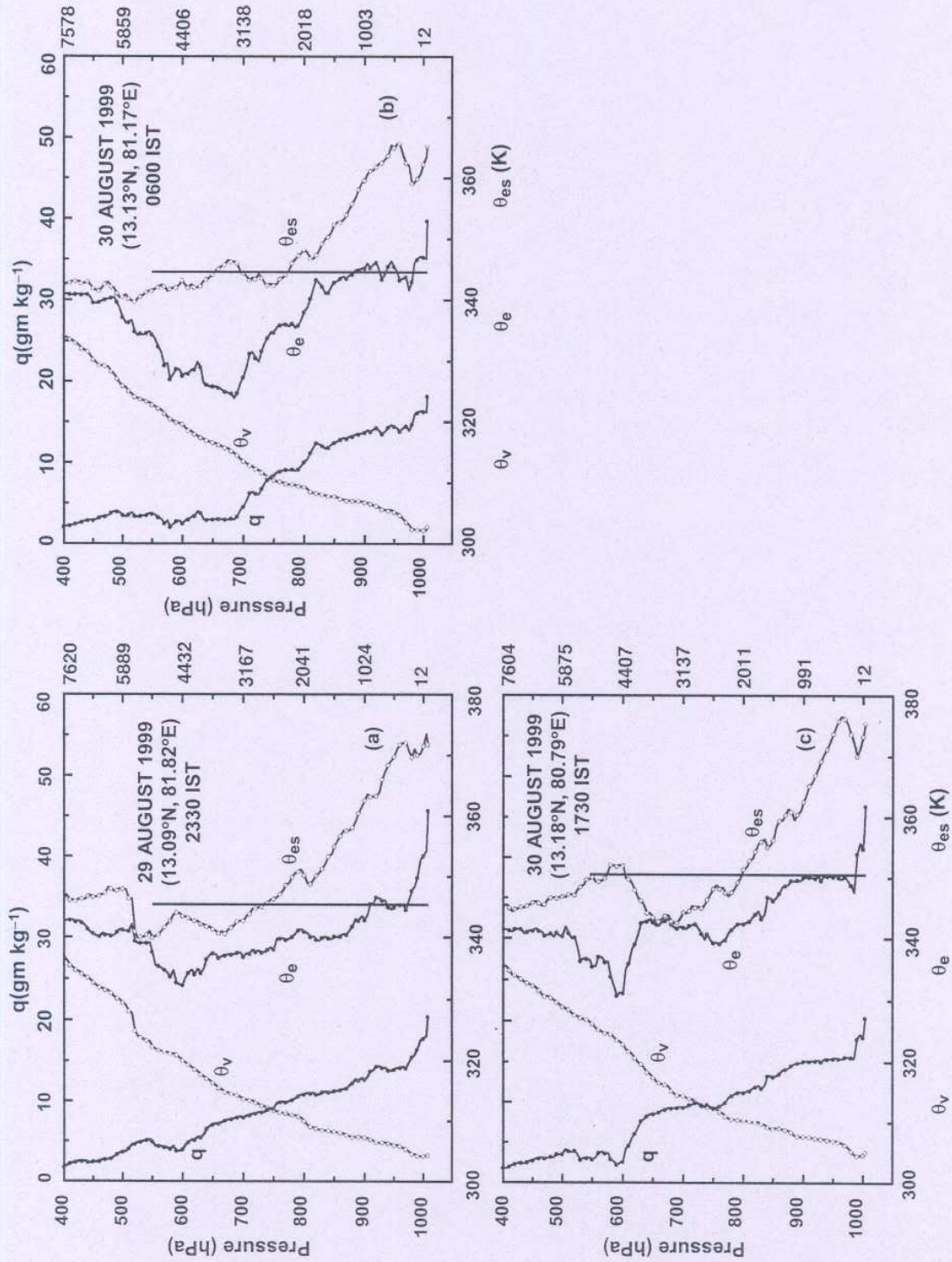| Regions	Region I						Region II				Region III		
August 1999	27			28			28	29			29	30	
Time (IST)	1130	1730	2330	0600	1130	1715	2330	0600	1130	1730	2330	0600	1730
Sur Pres.	1009.0	1006.8	1008.0	1006.2	1007.4	1005.5	1007.5	1005.9	1007.5	1005.3	1008.2	1006.8	1004.1
LCL Pres.	968.6	963.7	945.5	957.6	974.1	958.3	964.4	965.6	967.2	937.5	965.0	953.9	952.9
q at Sur.	20.9	20.1	19.1	20.4	19.8	19.3	20.3	20.5	21.0	18.5	20.4	18.2	20.4
q at 1000	17.3	18.4	18.1	18.0	17.3	17.4	17.9	19.3	17.0	16.5	17.8	16.3	18.4
T at LCL	25.8	24.3	23.0	25.4	23.6	23.7	24.5	24.4	23.3	24.4	26.8	25.3	27.0
θ_e at LCL	350.9	352.1	351.5	344.7	345.6	350.3	351.7	357.0	345.6	342.9	345.4	344.6	350.6
Sur layer	1000	1000	1005	1000	1000	1000	1000	1000	1005	1000	1000	1005	1000
Mixed layer	910	950	910	950	970	950	920	890	940	920	970	980	990
MABL top	660	700	820	710	750	710	770	540	720	770	600	680	590

Figure 4. Same as figure 3 but over region II.

Figure 5. Same as figure 3 but over region III.

top) and these levels were more or less coinciding with θ_{es} maxima as well. The levels of θ_e minima were at 980 and 680 hPa and the corresponding θ_{es} maxima were respectively at 960 and 670 hPa, thus the θ_e minima and the θ_{es} maxima differed by nearly 10–20 hPa in low levels (figure 5b). MABL top may be taken at 680 hPa in figure 5(b). In figure 5(c) the θ_e minima were observed at 990, 760 and 600 hPa and θ_{es} maxima occurred at 960, 750 and 590 hPa, similar to profiles in figure 5(b). The MABL top in figure 5(c) was at 590 hPa. The pressure 965.0, 953.9 and 952.9 hPa (table 1) respectively in figures 5(a), 5(b) and 5(c) describe the LCL heights over region III. The pseudoadiabats from these levels (LCL) on the θ_e profiles cut the θ_{es} curves at 730, 770 and 800 hPa respectively. Based on the comparison between the pseudoadiabat temperature and the θ_e curve, it is inferred that the convection was shallow over region III. There was stable stratification below 760 hPa and unstable stratification above this level.

4.3 *Conserved variable diagrams*

4.3.1 *Region I*

Figure 6(a–f) shows the θ_e–q profiles in region I. Of the six profiles shown in the figure, the profiles in figure 6(a), 6(e) and 6(f) were taken during overcast skies whereas the other three soundings (shown in figures 6(b), 6(c) and 6(d)) were taken during partly/less cloud times.

4.3.2 *Region II*

Figure 7(a–d) shows the θ_e–q diagrams for the overcast sky in region II. Figure 7(a) shows a couple of q reversal, one at 920 hPa and the other at 770 hPa which is the top of the MABL. Whereas the other three profiles show a weak q reversal at 890, 940 and 920 hPa levels respectively in figures 7(b), 7(c) and 7(d). The MABL tops in these three figures may be considered at 540, 720 and 770 hPa respectively.

4.3.3 *Region III*

Figure 8(a–c) shows the mixing line profiles of region III on the θ_e–q diagrams. All these profiles show multiple mixing lines. The saturation points cluster together on these mixing lines and these places are known as kinks as denoted by Betts and Albrecht (1987).

4.4 *Mean thermodynamic properties of the marine atmosphere along 13° N*

We have constructed mean vertical profiles of $q, \theta, \theta_v, \theta_e, p_{SL}, u$ and v components of wind in order to find the nature of vertical variation of these variables in each region.

4.4.1 *q and θ profiles*

Figure 9 (a and b) shows the mean vertical distribution of the specific humidity, $q(\text{gm kg}^{-1})$ and the potential temperature (θ, K) of the atmosphere over region I (solid line with open circle), region II (solid line with triangular symbol) and region III (solid line with solid circle) along 13°N from 87 to 80.79°E. Figure 9(a) shows that the mean q profiles in the three regions are similar from the surface to 400 hPa level. Near the surface below 990 hPa and above 520 hPa all the curves merge into one curve.

In figure 9(b), the θ profile of region I shows almost a linear trend without much variation with height whereas for regions II and III the θ profiles show fluctuations.

The mean potential temperature in the layer between surface to 990 hPa ($\sim$ 150 m layer thickness) is 300 K in all the three regions and is more or less similar to those of the tropical oceans elsewhere round the globe (Bates *et al* 1972). The mean pressure levels corresponding to the potential temperatures 310 K and 320 K respectively are 760 hPa and 590 hPa. The mean q value at 760 hPa is 9.5 gm kg^{-1} at all regions whereas the mean q at 590 hPa is 6 gm kg^{-1} in region I and region II and 2.5 gm kg^{-1} in region III (which is almost dry in this region). The thickness of the layer is about 170 hPa (760 to 590 hPa) which is about 1700 m thick and is the same as the standard layer as reported by Bates *et al* (1972) over the tropical oceans.

4.4.2 *θ_v profiles*

Figure 10 (a and b) shows the average vertical profiles of θ_v–p (pressure) and θ_v–p_{SL} (saturation level pressure) for regions I (solid line with open circle), II (solid line with solid triangle) and III (solid line with solid circle). It is seen from figure 10(a) that the θ_v profiles of regions I and III have a similar slope and trend as those of the θ profiles and they are independent of q profiles. This implies that there is a little effect of q on θ_v as compared to θ. The θ_v shows a sharp decrease with height from surface to 1000 hPa and then near-isothermal (conserved) between 1000 and 960 hPa in regions I and II and from 1000 to 980 hPa in region III. The other changes in the curves are more or less similar to θ profiles in figure 9(b).

4.4.3 *u and v components of wind*

Figure 11 shows the vertical distribution of the mean u and v components of the wind field over
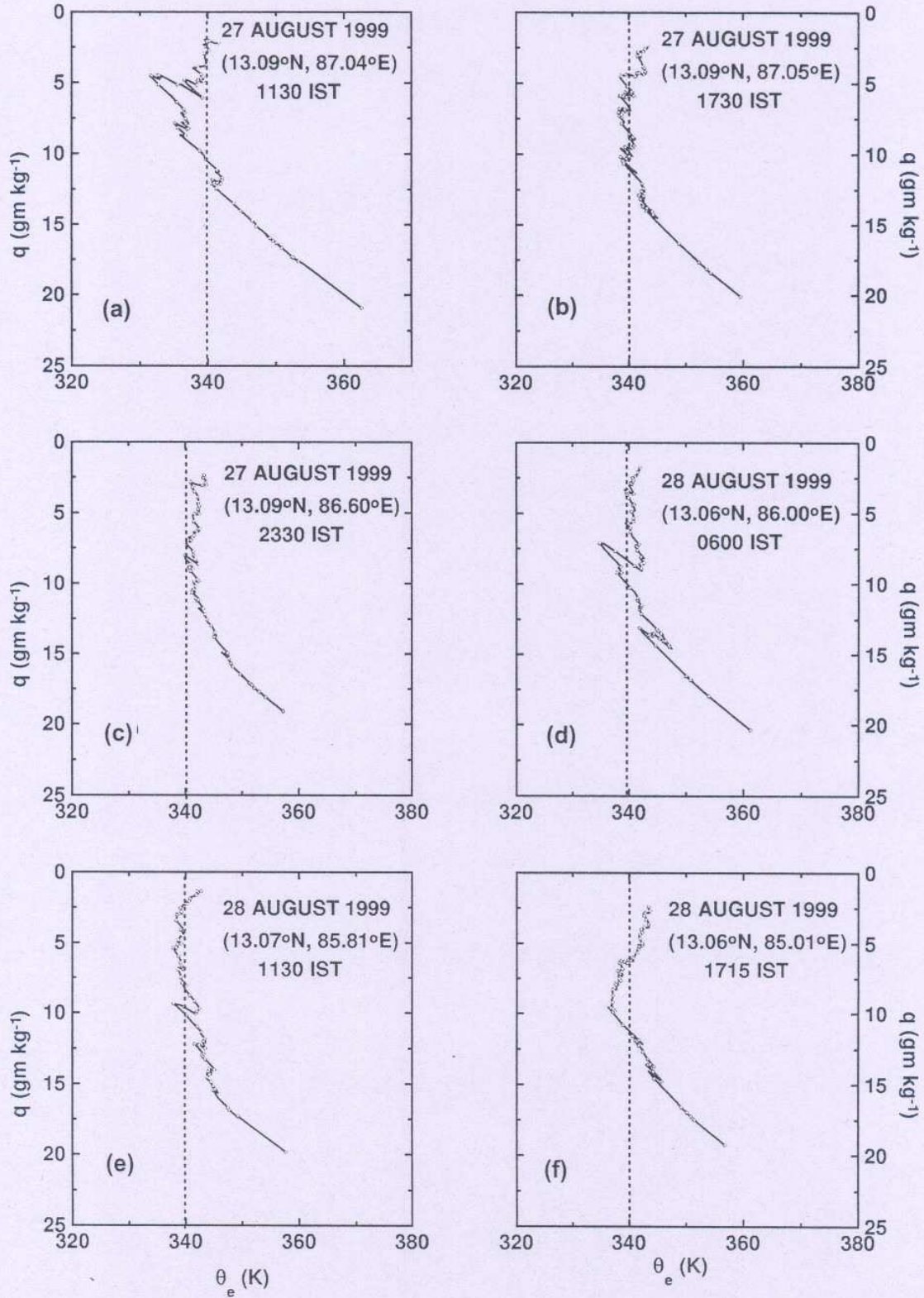
Figure 6. Conserved variable diagrams (θ_e, q) for the 6-hourly radiosonde ascents over region I. The vertical dashed line is drawn at $\theta_e = 340$ K.
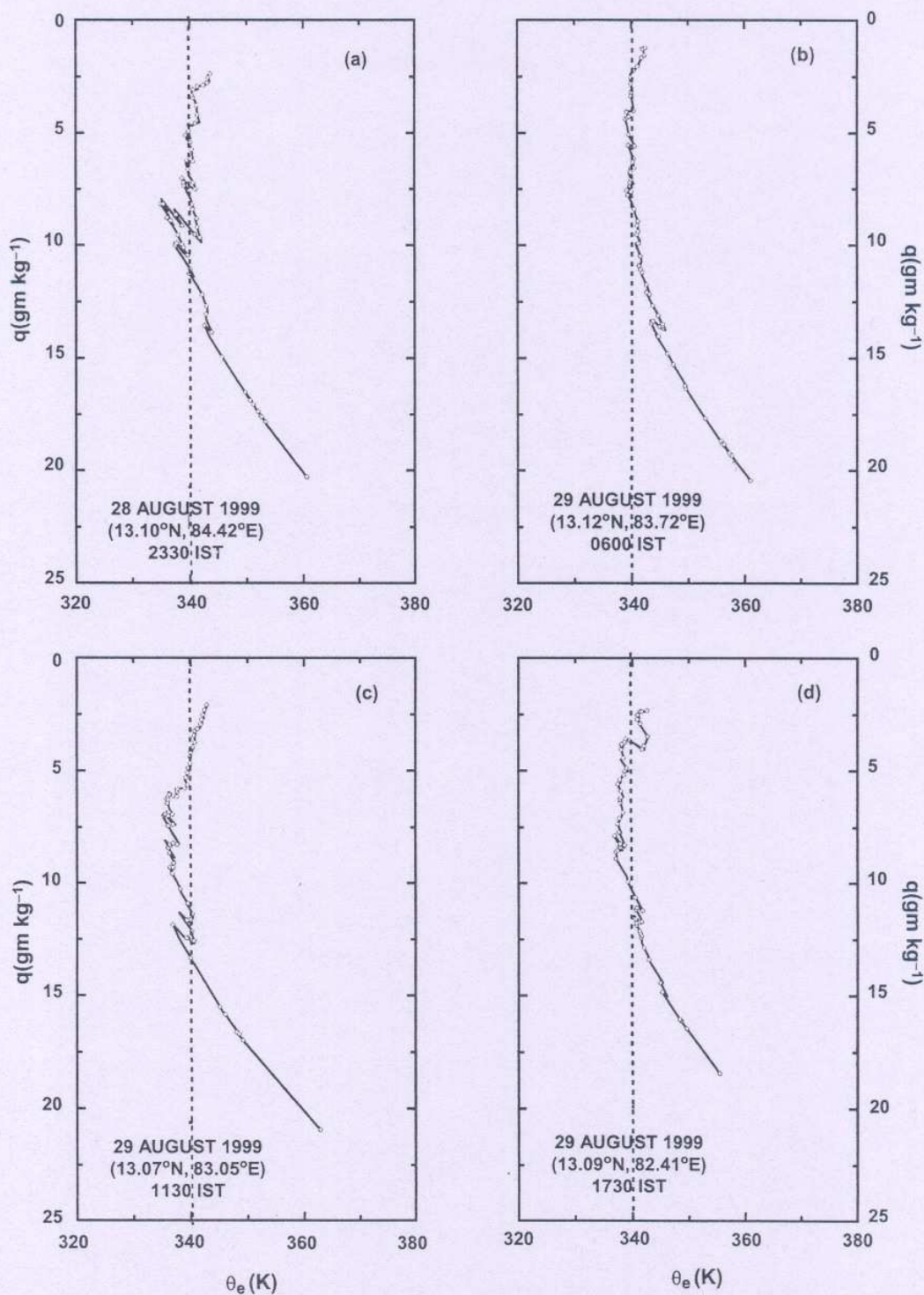
Figure 7.   Same as figure 6 but over region II.

regions I to III. The u component is positive throughout the depth of the atmosphere (surface to 400 hPa) over all the three regions. This indicates that at the time when these observations were made the southwest monsoon current was having a strong westerly component. The magnitude of the v component varied between -3 and $+3$ m s^{-1} from 950 to 400 hPa levels. Below 950 hPa the values
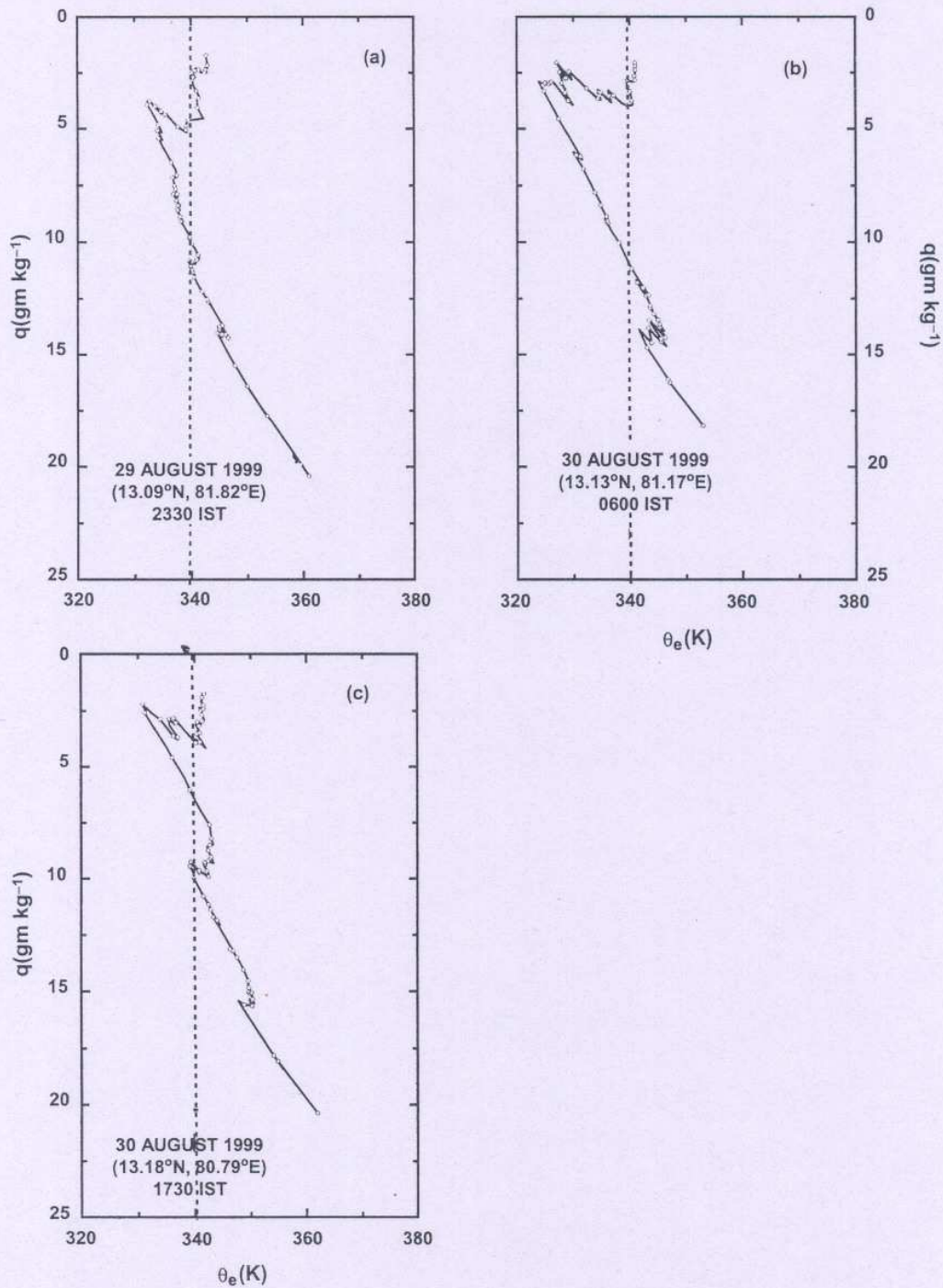
Figure 8. Same as figure 6 but over region III.

were greater than $4\,\mathrm{m\,s^{-1}}$ around 970 hPa. Also, above 500 hPa only in region II the values of v component were greater than $6\,\mathrm{m\,s^{-1}}$ near 430 hPa level. The v component in region III was negative (i.e., northerly) between 900 and 500 hPa levels. In region II it assumes negative values at 800 and 760 hPa levels whereas in region I it is negative at 450 hPa.
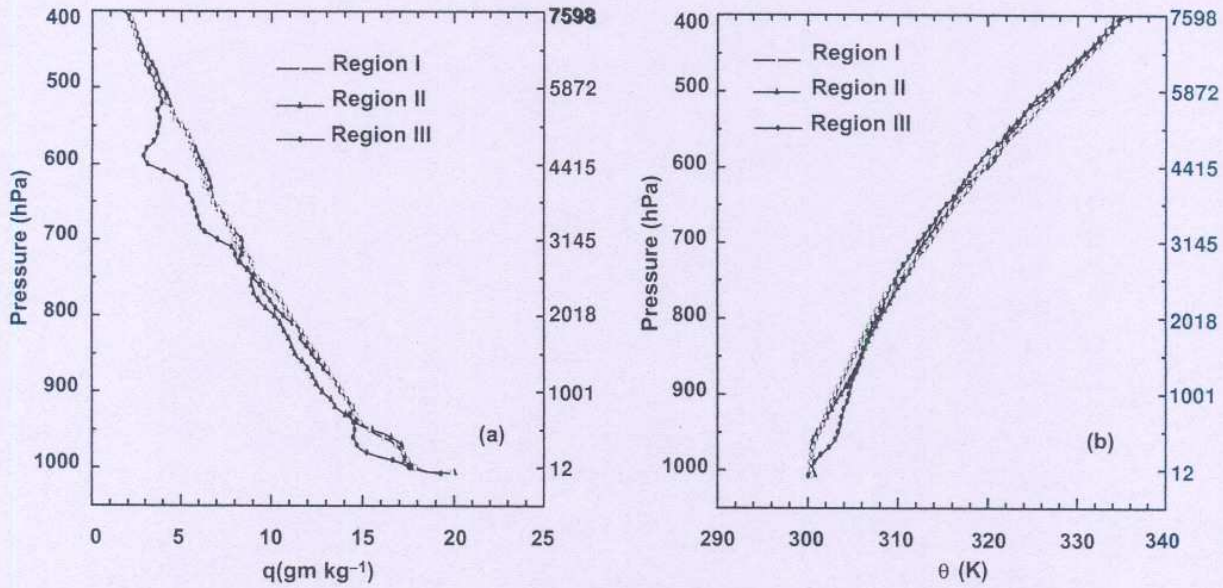
Figure 9.   Mean vertical profiles of (a) mixing ratio (q) and (b) potential temperature (θ) for regions I, II and III during 27th–30th August 1999. In each figure on the Y-axis pressure levels are marked on the left side and the corresponding heights are indicated on the right side.
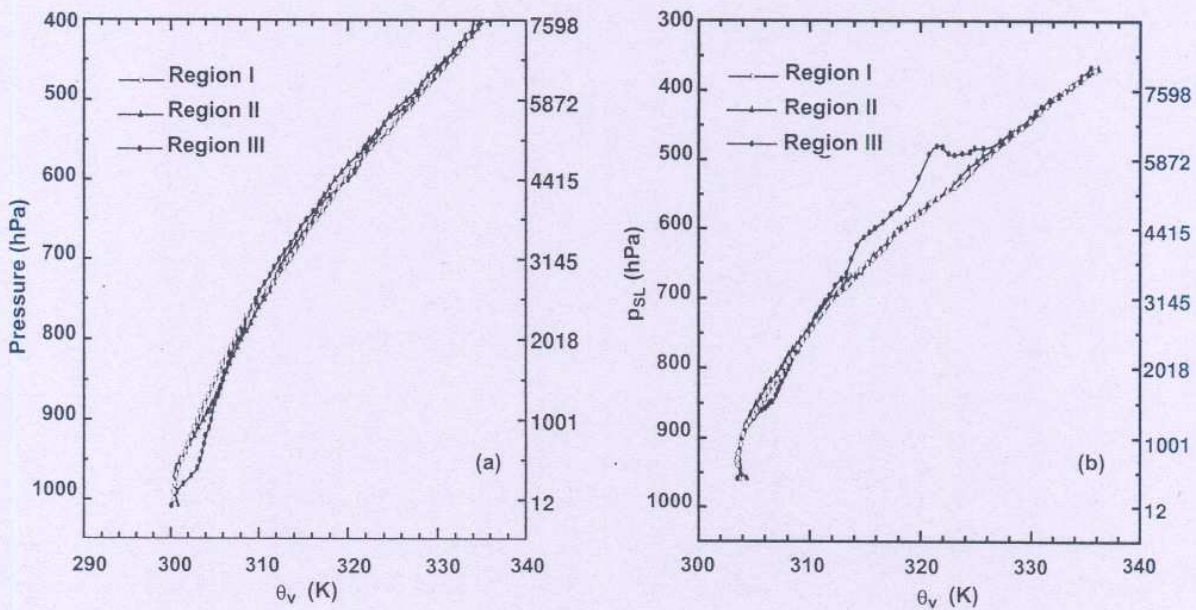

Figure 10.   (a) Mean vertical profile of virtual potential temperature (θ_v) and (b) profile of mean virtual potential temperature (θ_v) against mean saturation pressure (p_{SL}) for regions I, II and III during 27th–30th August 1999. In both the figures on the Y-axis pressure levels are marked on the left side and the corresponding heights are indicated on the right side.
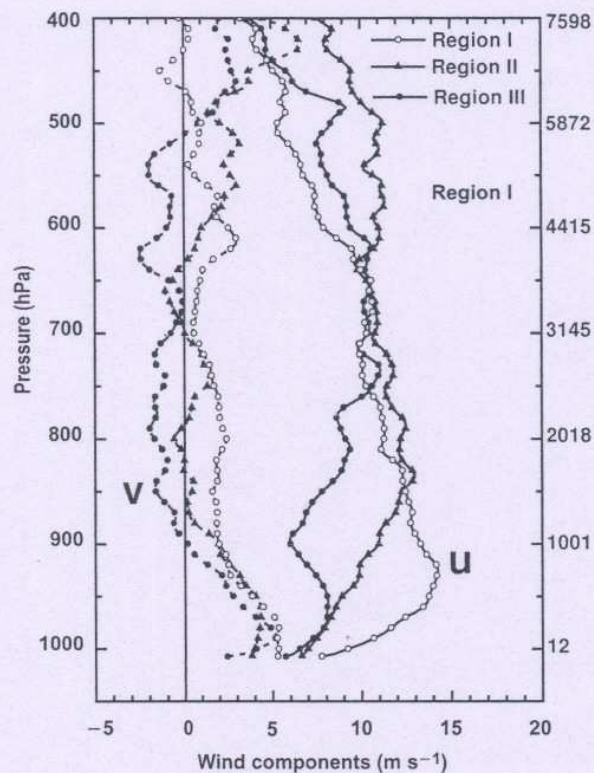
Figure 11. Mean vertical profiles of u and v components of wind for regions I, II and III during 27th – 30th August 1999. On the Y-axis pressure levels are marked on the left side and the corresponding heights are indicated on the right side.

5. Concluding remarks

The thermodynamic properties of the marine atmosphere (surface to 400 hPa) along 13°N (80.79–87°E) in the Bay of Bengal during the period 27th – 30th August, BOBMEX-99, were studied using 13 high (5 hPa) resolution radiosonde profiles and surface meteorological observations. The above period was characterized by bad weather due to monsoon disturbances (well marked low pressure area) over the head of the Bay of Bengal close to the north Orissa coast (figure 1). We divided the area of observation into three regions (region I, region II and region III) according to the nature of pressure distribution and the total cloud amount. The 13 radiosondes we examined can be divided into three groups each belonging to one of the three regions. In the first group there are 6 radiosondes and is confined to region I (85°–87°E, low pressure, partly cloudy sky, open ocean). The second group consists of 4 radiosonde ascents confined to region II (85–82°E, overcast sky and influenced by marine as well as continental atmosphere) and the third group containing three radiosondes is confined to region III (82–80.79°E, partial overcast sky and close to coast, continental atmosphere). In

region I, θ_e and θ_{es} profiles showed stable layers in the lower marine atmospheric boundary layer and medium clouds between 850 and 500 hPa. In region II, they showed low level stability and upper level instability, θ_e was nearly constant with height above 800 hPa, implying falling precipitation at the time of observations. In region III too, θ_e and θ_{es} curves showed low level stability with formation of shallow clouds in the middle troposphere. Double mixing line structure was evident from all the θ_e–q diagrams. The fluctuations observed in the vertical profiles of mixing ratio (q), potential temperature (θ) and virtual potential temperature (θ_v), in general, in the layer 990–520 hPa, were minimum in region I, intermediate in region II and maximum in region III. The vertical profiles of the above thermodynamical parameters in all the regions approximately merge into one profile below 990 hPa and above 520 hPa. The mean vertical profiles of saturation pressure deficit (P^*), equivalent potential temperature (θ_e) and saturated equivalent potential temperature (θ_{es}) indicated that the MABL top in regions I, II and III can be considered at the levels 710, 650 and 590 hPa respectively. The structure of these profiles is in agreement with those of Bates *et al* (1972).

The wind profiles indicated the advection of continental air mass (mostly warm and dry in region III) to the adjacent oceanic regions i.e., regions II and III (relatively cold and moist air mass). However, region I, which is over the open ocean, was hardly affected by the land air mass. The LCL heights varied from 981 to 946 hPa and were found to be above 963 hPa in region I and below 963 hPa over regions II and III. Mixed layer heights based on constancy of θ_v varied between 910 and 980 hPa in general. The SST and air temperature showed variation in the range of 28.2–28.7°C and 26.2–29.6°C respectively over the observational area.

Acknowledgement

List of Symbols

T Temperature (°C).

T_d Dew point temperature (°C).

p Air parcel pressure (hPa).

u Zonal component of wind (m sec^{-1}).

v Meridional component of wind (m sec^{-1}).

dd Wind direction (degrees).

ff Wind speed (m sec^{-1}).

q Mixing ratio (gm kg^{-1}).

θ Potential temperature (K).

θ_v Virtual potential temperature (K).

θ_e Equivalent potential temperature (K).

θ_{es} Saturated equivalent potential temperature (K).

P^* Saturation pressure deficit (hPa).

p_{SL} Pressure at saturation level (hPa).

θ_{SL} Potential temperature at saturation level (K).

q_{SL} Mixing ratio at saturation level (gm kg^{-1}).

LCL   Lifting condensation level (hPa).

CA   Cloud amount (octa).

References

Bates J R, Wobus R and Young J A 1972 Thermodynamic variables, tropical sounding and instability; *Notes from a colloquium: Summer 1972 on dynamics of the tropical atmosphere*, NASA, Boulder, Colorado, pp. 463–468

Betts A K 1982 Saturation point analysis of moist convective overturning; *J. Atmos. Sci.* **39** 1484–1505

Betts A K and Albrecht B A 1987 Conserved variable analysis of the convective boundary layer thermodynamic structure of the tropical oceans; *J. Atmos. Sci.* **44** 83–99

Bhat G S 2001 The variation of CAPE and CINE during BOBMEX; *Proc. TROPMET-2000 national symp. on tropical meteorology*, pp. 382

Bhat G S, Ameenulla S, Venkataramana M and Sengupta K 2000 Atmospheric boundary layer characteristics during BOBMEX-Pilot experiment; *Proc. Indian Acad. Sci. (Earth Planet. Sci.)* **109** 229–237

Bhat G S, Gadgil S, Hareesh Kumar P V, Kalsi S R, Madhusoodanan P, Murty V S N, Prasada Rao C V K, Ramesh Babu V, Rao L V G, Rao R R, Ravichandran M, Reddy K G, Sanjeeva Rao P, Sengupta D, Sikka D R, Swain J and Vinayachandran P N 2001 BOBMEX: The Bay of Bengal Monsoon Experiment; *Bull. Am. Meteorol. Soc.* **82** 2217–2243

Haltiner G J and Martin F L (ed) 1957 *Dynamical and physical meteorology*, McGraw-Hill Book Company, pp. 470

Hastenrath S and Lamb P J 1979 *Climatic atlas of the Indian Ocean, Part-I, Surface climate and atmospheric circulation.* (USA: The University of Wisconsin Press)

Kloesel K A and Albrecht B A 1989 Low-level inversions seen over the tropical Pacific – thermodynamic structure of the boundary layer and the above inversion moisture structure; *Mon. Weather Rev.* **117** 87–101

Morwal S B 1998 Nature and some evolutionary aspects of the monsoon boundary layer; *Ph.D. thesis*, pp. 213

Morwal S B 2000 Convective boundary layer structure over the equatorial Indian oceanic region; *Mausam* **51** 169–176

Seetaramayya P, Tyagi Ajit and Nagar S G 2001 Thermodynamic structure of the marine atmosphere over the southern Bay of Bengal during BOBMEX-98; *Proc. TROPMET-2000 national symp. on tropical meteorology* (ed) P V Joseph and others, Indian Meteorological Society, pp. 385

Sikka D R and Sanjeeva Rao P 2000 Bay of Bengal Monsoon Experiment (BOBMEX) – A component of the Indian Climate Research Programme (ICRP); *Proc. Indian Acad. Sci. (Earth Planet. Sci.)* **109** 207–210

Swain J, Prasada Rao C V K, Hareesh Kumar P V, Shukla R K, Unny V K, Mohan Kumar N and Raghunadha Rao R 2001 Observed wind and wave characteristics in the south central Bay of Bengal during BOBMEX-99; *Proc. TROPMET-2000 national symp. on tropical meteorology* (ed) P V Joseph and others, Indian Meteorological Society, pp. 406

Venkata Ramana M, Sen Gupta K, Radhika Ramachandran, Sudha Ravindran, Ameenulla S and Raju J V S 1999 Latitude variation of boundary layer height over Indian Ocean during pre- and First Field Phase (FFP-98) of INDOEX; *Curr. Sci.* **76** 898–902